Copyright Warning & Restrictions

The copyright law of the United States (Title 17, United States Code) governs the making of photocopies or other reproductions of copyrighted material.

Under certain conditions specified in the law, libraries and archives are authorized to furnish a photocopy or other reproduction. One of these specified conditions is that the photocopy or reproduction is not to be "used for any purpose other than private study, scholarship, or research." If a, user makes a request for, or later uses, a photocopy or reproduction for purposes in excess of "fair use" that user may be liable for copyright infringement,

This institution reserves the right to refuse to accept a copying order if, in its judgment, fulfillment of the order would involve violation of copyright law.

Please Note: The author retains the copyright while the New Jersey Institute of Technology reserves the right to distribute this thesis or dissertation

Printing note: If you do not wish to print this page, then select "Pages from: first page # to: last page #" on the print dialog screen

ABSTRACT

SYNTHESIS AND CHARACTERIZATION OF SILICON DIOXIDE THIN FILMS BY PLASMA ENHANCED CHEMICAL VAPOR DEPOSITION FROM DIETHYLSILANE AND NITROUS OXIDE

by
Lan Chen

This study is focused on the synthesis and characterization of silicon dioxide thin films deposited on silicon wafers by plasma enhanced chemical vapor deposition(PECVD), using diethylsilane (DES) as a precursor and nitrous oxide (N_2O) as the oxidant. The process parameters, such as temperature, pressure and reactant gas composition have been systematically varied and their effects on the film growth rate and properties were investigated. The growth rate was found to be inversely proportional to the temperature in the examined range of 100-300^{0}C. It increased with increasing N_2O/DES flow rate ratio as the total flow rate increased from 135 to 315 sccm, and also increased with the chamber pressure and saturated. The optimized deposition condition appeared to be at 300^{0}C, 300mTorr, and a flow rate ratio N_2O/DES = 240 sccm/15 sccm. For these conditions, the films were found to have a high growth rate of 327Å/min with density of 2.14g/cm^3 and refractive index of 1.47.

SYNTHESIS AND CHARACTERIZATION OF SILICON DIOXIDE THIN FILMS BY PLASMA ENHANCED CHEMICAL VAPOR DEPOSITION FROM DIETHYLSILANE AND NITROUS OXIDE

by
Lan Chen

A Thesis
Submitted to the Faculty of
New Jersey Institute of Technology
in Partial Fulfillment of the Requirements for the Degree of
Master of Science in Applied Chemistry

Department of Chemical Engineering, Chemistry
and Environmental Science

October 1995

APPROVAL PAGE

SYNTHESIS AND CHARACTERIZATION OF SILICON DIOXIDE THIN FILMS BY PLASMA ENHANCED CHEMICAL VAPOR DEPOSITION FROM DIETHYLSILANE AND NITROUS OXIDE

Lan Chen

Dr. James M. Grow, Thesis Advisor — Date
Professor of Chemical Engineering, Chemistry and
Environmental Science, NJIT

Dr. Roland A. Levy, Thesis Advisor — Date
Professor of Physics,
Director of Material Science and Engineering Program, NJIT

Dr. Lev N. Krasnoperov — Date
Professor of Chemical Engineering, Chemistry and
Environmental Science, NJIT

BIOGRAPHICAL SKETCH

Author: Lan Chen

Degree: Master of Science in Applied Chemistry

Date: October, 1995

Undergraduate and Graduate Education:

- Master of Science in Chemistry,
  New Jersey Institute of Technology,
  Newark, New Jersey, 1995

- Master of Science in Chemistry,
  Wuhan University,
  Wuhan, P.R. China, 1993

- Bachelor of Science in Environmental Chemistry,
  Wuhan University of Hydraulic and Electric Engineering,
  Wuhan, P.R. China, 1990

Major: Applied Chemistry

This thesis is dedicated to
my dear parents

ACKNOWLEDGMENT

The author wishes to express her sincere gratitude to her advisors, Professor James M. Grow and Professor Roland A. Levy, for their guidance, inspiration, and support thoughout this research.

Special thanks to Professor Lev N. Krasnoperov for serving as a member of the thesis committee.

The author appreciates the timely help and suggestions from the CVD laboratory memberes, including: Vitaly Sigal, Dr. Jan Opyrchal, Mahalingam Bhaskaran, David Perese, Emmanuel Ramos, Hongyu Chen, Manish Narayan, Chenna Ravindranath. Also thanks Scott Margo for the measurement of hardness and Young's modulus.

TABLE OF CONTENTS

TABLE OF CONTENTS
(Continued)

LIST OF TABLES

LIST OF FIGURES

LIST OF FIGURES
(Continued)

Figure **Page**

LIST OF FIGURES
(Continued)

CHAPTER 1

INTRODUCTION

1.1. Applications of SiO_2 Thin Films

Silicon dioxide is an important material in the fabrication of microelectronics circuits. It provides protection to semiconductor surfaces to serve as implantation or diffusion masks, or as interlayer dielectronics between two levels of metalization, and for many other applications. The success of silicon integrated circuits, from low packing density devices, through large scale integrated circuits, very large scale integrated circuits and ultra large scale integrated circuits lies in the successful growth of films on silicon. SiO_2 satisfies almost all the requirements of a dielectric film for multilevel metalization and passivation layers, which includes[1]:

Intermetal dielectric

1) low dielectric constant to keep the capacitance between metal lines at a minimum;
2) high dielectric break down field strengths;
3) low moisture absorption;
4) low compressive stress;
5) good adhesion to aluminum;

6) capability of being easily dry or wet etched;

7) being permeable to hydrogen to remove interface sites;

8) good conformal step coverage.

Passivation layers

1) capability of providing scratch protection to circuit below;

2) zero permeability to moisture;

3) low compressive stress;

4) good conformal step coverage;

5) being easily patterned;

6) good adhesion to conductors and interlayer dielectrics.

The principal physical properties of SiO_2 are given in Table 1.1 [2].

Recently, a new application of SiO_2 as a composite/ceramic membrane for gas-separation has been developed by depositing the material on a microporous substrate to reduce the pore size and thus to achieve particular selectivity of the porous membranes [3]. Silicon dioxide is a competitive material for this technology because of its inherent properties such as thermal stability, corrosion resistance, and also due to the fact that the difference in thermal expansion coefficients between the ceramic substrate and SiO_2 deposit is very low.

Table 1.1 Physical Properties of Silicon Dioxide

melting point	1728^{0}C
boiling point	2950^{0}C
heat capacity	0.185 cal/g 100^{0}C
Si-O bond distance	1.62 Å
density	2.1975 g/cm^3 (0^{0}C)
Mohr's hardness	7.7GPa
refractive index	1.4584 (5893Å)
Young's modulus	10.5 x 10^6 psi

1.2 Chemical Vapor Deposition Techniques

1.2.1 Fundamental Aspects of Chemical Vapor Deposition

Chemical Vapor Deposition (CVD) is one of the most popular techniques of growing a very thin film on various substances. The reason for its promising applications lies in its versatility for depositing a very large variety of materials at relatively low temperatures [1].

Chemical Vapor Deposition (CVD) is defined as the formation of a non-volatile solid film on a substrate by the reaction of vapor phase chemicals (reactants) that contain the required constituents. The reactant gases are

introduced into a reaction chamber and are decomposed and reacted at a heated surface to form the thin film.

Thin films used in a host of different applications in VLSI fabrication must exhibit the following characteristics: 1) good thickness uniformity; 2) high purity and density; 3) controlled composition and stoichiometries; 4) high degree of structure perfection; 5) good electrical properties; 6) excellent adhesion; 7) good step coverage. CVD films synthesized under optimized conditions can satisfy these requirements.

The procedure of Chemical Vapor Deposition involves flowing a reactive gas or gas mixture over a surface that catalyzes a chemical reaction to form a solid product[4]. CVD reactions can be homogeneous, heterogeneous or a combination of both. Homogeneous reactions nucleate in the gas phase and lead to particle formation, which can result in low density films, poorly adhering, or defects in the depositing films. In addition, such reactions also consume reactants and can cause decrease in deposition rates[1]. Heterogeneous reactions are generally favored because they take place at the substrate surface rather than in the gas phase and form desirable good quality film deposit. One important characteristic of a chemical reaction for CVD application is the degree to which heterogeneous reactions are favored over gas phase reactions. A typical CVD process consists of at least the following steps [5]:

Arrival

1. bulk transport of the reactants and diluent inert gases into the reaction chamber;
2. gaseous diffusion of the reactants to the substrate surface;
3. adsorption of the reactants on the surface;

Surface reaction

4. surface diffusion of the reactants;
5. chemical reaction of the adsorbed reactant molecules;

Removal of reactant by-products

6. desorption of the reactant by-products;
7. gaseous diffusion of the reactant by-products;
8. bulk transport of the by-products and unreacted gases out of the reaction chamber.

Thermally-driven CVD reactions are dynamical equilibrium processes. There is a typical temperature dependence of deposition rate sketched in Figure 1.1[6]. At low temperature the reaction is generally surface reaction controlled, while at high temperature, it is usually limited by mass transfer.

If the process is controlled by the surface reaction, i.e. reaction rate is limited by the rate of surface reaction, the deposition mechanism of the solid film follows the empirical Arrhenius behavior [5, 6]:

$$D.R. = A \exp(- E_a / RT) \quad (1.1)$$

where ,

D.R. is the deposition rate of the film;

E_a is the apparent activation energy of the chemical reaction;

R is the gas constant;

T is absolute temperature (K);

A is constant.

According to this equation, the reaction rate increases with the increasing temperature. There is a linear plot of ln(D.R) vs. 1/T.

When the temperature rises high enough and the reaction rate approaches the rate of the reactant species arriving at the surface, the reaction rate can not increase any more, unless there is an increase in the rate at which the reactant species are supplied to the surface by diffusion and mass transport. In this case, the reaction is mass transport controlled. The reaction rate can then be expressed as below:

$$D.R. = s\, k_D / RT\, (P - P_0) \quad (1.2)$$

where,

s is surface area of the substrate;

k_D is mass transport coefficient;

P is partial pressure of the reactant;

P_0 is equilibrium partial pressure of the reactant at certain temperature;

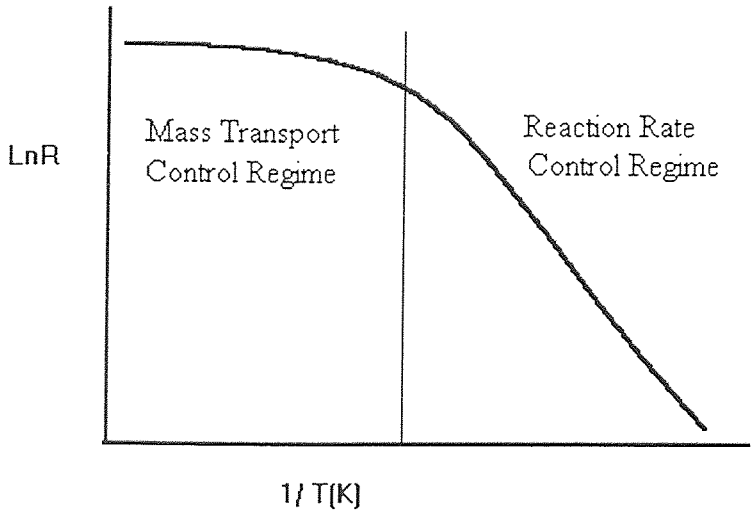

Figure1.1 Temperature Dependence of Deposition Rate

The critical temperature at which the reaction mechanism is switched from one rate-controlling regime to another is associated with the activation energy and the gas flow conditions. Adsorption of decomposition products on the surface of the substrate may be an additional factor retarding film growth.

For those processes in which heat is not the predominant energy source, such as plasma-enhanced CVD, the reactions are non-equilibrium. The mechanism of the reaction is complex, since there are many excited species,

e.g., radicals, atoms, ions produced by electron impact and unexcited gas molecules as well. Upon being adsorbed on the substrate, these species are subjected to ion and electron bombardment, rearrangements, reactions with each other, new bond formations and film growth[1]. Such that the relationship between deposition rate and temperature is not like what was stated above. However, temperature is still an important factor affecting the CVD process and the properties of the deposits as well.

Consequently, the deposition rate and the properties of the CVD film depend on the deposition conditions, such as reaction temperature, pressure, reactant flow rates, power density (as in plasma-enhanced CVD process) and so on. Studies on the effects of such variables will result in good understanding of the CVD processes.

1.2.2 Categories of CVD

The energy to activate and drive the chemical processes can be thermal, supplied by an electric glow discharge plasma, or attained by electromagnetic radiation (usually ultraviolet or laser radiation). According to the type of energy supplied to initiate and sustain the reaction, CVD processes can be classified into following categories [7]:

1) Thermally activated reactions at various pressure ranges; which comprise the vast majority of CVD processes. Heat is applied by resistance heating, rf inducting heating , or infrared radiation heating techniques.

2) Plasma promoted reactions, where an rf or dc induced glow discharge is the source for most of the energy that initiates and enhances the rate of reaction, usually called plasma-enhanced CVD (PECVD).

3) Photo induced reactions, where a specific wavelength radiation triggers and sustains the reaction by direct photolysis or by an energy transfer agent .

The most important and widely used CVD processes are atmospheric pressure CVD (APCVD), low pressure CVD (LPCVD) and plasma enhanced CVD (PECVD). A general description of APCVD and LPCVD will be made below and PECVD as the technique employed in this study will be discussed in detail.

1.2.2.1. Atmospheric Pressure CVD (APCVD): Much of the early CVD development work was done by APCVD. It offered such advantages as operation without the need for a vacuum system, high dilution of toxic or flammable gases, and the potential for operation as continuous-feed belt systems. Disadvantages of APCVD operation included the need for large volumes of carrier gas, large size, and high levels of particulate contamination. In recent years, atmospheric operation have faded from popularity, with most significant developments occurring in the remaining two categories.

1.2.2.2. Low Pressure CVD (LPCVD): In low pressure CVD processes [8-14], the reduced gas pressure enhances the mass transfer rate relative to the

surface reaction rate, this makes it possible to deposit film uniformly in a relative highly economical close spaced positioning of the substrate wafers in a standup fashion [8].

The outstanding advantage of LPCVD technique lies in the thickness uniformity of the films and the step coverage which are substantially improved over those obtained in conventional atmospheric pressure CVD reactors. The films have fewer defects, such as particulate contaminants and pinholes, because of the inherently cleaner hot wall operations and the vertical wafer positioning that minimize the formation and codeposition of homogeneously gas phase nucleated particles [14]. These considerations are especially important in VLSI processing where a very high device reliability and high product yield must be achieved.

The drawbacks of the LPCVD is the need of relatively high temperature (550-850^{0}C) and relatively low deposition rate.

1.2.2.3. Plasma-Enhanced CVD (PECVD): Plasma deposition is a combination of a glow discharge process and low pressure chemical vapor deposition in which highly reactive chemical species are generated from gaseous reaction by a glow discharge and interact to form a thin solid film product on the substrate and electrode surface [7]. Since the plasma assists or enhances the CVD reaction, the process is denoted as Plasma-Enhanced CVD (PECVD).

Plasma-enhancement offers an alternative to thermal energy for initiating chemical reactions leading to film deposition. Use of plasma frequently allows deposition at a much lower temperature than could otherwise be achieved, and/or it permits the use of source gases that would ordinarily be considered unreactive. This is the major advantage of PECVD. Radicals, which are predominant species in plasma field, tend to have high sticking coefficients, and also appear to migrate easily along the surface after adsorption. These two factors can lead to excellent film conformality. Another benefit is very high growth rate, although, care must be taken to minimize stresses and contaminations[7]. Desirable film properties such as good adhesion, low pinhole density, good step coverage, adequate chemical properties can also be obtained by PECVD superior to those of APCVD or LPCVD films. Moreover, the mechanical strength of plasma deposited films is excellent due to their intrinsic compressive stress and high film density [15,16]. However, the complexity of reactions associated with PECVD makes the synthesis of stoichiometric composition difficult. And, as a consequence of the low temperature for film formation, gases are trapped in the films, which frequently causes thermal instability due to outgasing. Though sensitive MOS devices may be damaged by the radiation associated with the plasma discharge, the damage can usually be eliminated by a thermal anneal at the deposition temperature[4].

The main factors which affect the PECVD processes and the thin film properties include plasma power density, frequency as well as the substrate

temperature and partial pressure of reactant gases, etc.

1.3 Chemical Vapor Deposition of SiO_2

SiO_2 film can be deposited by CVD in several ways, depending on the specific applications. The temperature ranges in which CVD SiO_2 film can be formed are: 1) low temperature deposition, 300-450^{0}C; medium temperature deposition, 450-800^{0}C; and 3) high temperature deposition, above 800^{0}C .

Although excellent uniformity films and properties close to thermally grown oxide can be obtained by the reaction of dichlorosilane and nitrous oxide at 900^{0}C[17,18], the high temperature prohibit the application of such approaches for deposition over aluminum-based conductors.

In the lower temperature range, most of the early processes were based on the silane chemistry :

$$SiH_4(g) + O_2(g) \text{ ====> } SiO_2(s) + 2H_2(g) \qquad (1.1)$$

The deposition can proceed in atmospheric pressure (APCVD) reactors [19-21], low pressure CVD (LPCVD) reactors [22-36], or plasma-enhanced CVD (PECVD) [37-44] .

APCVD employs a simpler and less expensive system, which is the main advantage over other ones that require a vacuum environment. Because rates as large as 100nm/min were readily attained [19,20], such reactors achieved

very good throughput. Operation at atmospheric pressure, however, lends to the danger of homogeneous gas phase nucleation which produced unacceptably high levels of defects, unless a high degree of inert gas diluent is used.

LPCVD produced cleaner films due to a reduction in gas phase nucleation. But the deposition rate based on the same chemistry (Equation (1.1)) was found to be as low as 2-4 nm/min where the system throughput was not competitive though excellent uniformity of film thickness and composition were obtained [18].

SiO_2 films can also be deposited by plasma enhanced CVD (PECVD) in the low temperature range with high growth rate and good properties.

1.3.1 PECVD of SiO_2 from Silicon

The oxidation of silicon in an oxygen plasma allowed the controlled growth of thin, high-quality films of SiO_2 at temperatures down to room temperature in a clean vacuum environment[49]. The rate of oxidation and electrical properties may vary greatly depending upon the oxidation conditions. Plasma ion density and sample temperature are the two important factors affecting growth. The reported physical properties of the plasma-grown oxide films, including density and refractive index, were found to be indistinguishable from thermally grown oxides. The P-etch rate was found to be similar to that of thermal oxides.

1.3.2 PECVD of SiO_2 from Silane

In this process, nitrous oxide(N_2O) was used as the oxidant instead of O_2[23, 37, 40, 50, 51]. A typical reaction would be :

$$SiH_4 + N_2O \text{ ====> } SiO_2 + 2H_2 + 2N_2 \qquad (1.2)$$

The process can be carried out between 200-400^{0}C. The PECVD SiO_2 films are known to contain hydrogen as well as nitrogen, and to have a high etch rate, high refractive index, low stress (usually compressive) and to be oxygen deficient. Conformal coated, low pinhole count and excellent adhesion films were obtained by this technique [37].

Optimized gas composition of N_2O/SiH_4 ratio 40-60 and rf power density 0.05W/cm^2 were employed to suppress gas phase reactions and enhance surface reactions. A typical deposition rate of 60 nm/min was readily obtained at 300^{0}C[40]. High refractive index (1.54) may be ascribed to the slightly excess of silicon in the film.

Chapple-Sokol etc.[51] found that susceptor temperature had a more significant effect on the impurity levels in the film while increase rf power density yielded oxides which were structurally more relaxed and homogenous. The combination of elevated power density with increased susceptor temperature resulted in the deposition of films of high physical integrity when SiO_2 films were

deposited from silane and nitrous oxide in the presence of large excess of helium(80-99% of the total gas flow) [50].

The correlationships between the film composition and properties along with the relationships between the deposition parameters and film composition were studied by Ceiler etc.[51]. They examined the effects of the deposition parameters on the properties when SiO_2 was deposited by PECVD from silane and nitrous oxide at low temperature (200-400 ^{0}C), using nitrogen as a diluent gas.

1.3.3 PECVD of SiO_2 from TEOS

Tetraethoxysilane(TEOS) was utilized as a chemical source of PECVD SiO_2 films in place of silane , using oxygen or nitrous oxide as an oxidant[37-42]. Regardless of the oxidant, a substantial improvement of the step coverage of the film was obtained, compared to what was obtained for oxide films deposited using silane-based chemistry. Contrary to the silane-based process, temperature has a significant effect on the deposition rate and wet etching rate, i.e., densification state of the oxide film. A decrease in the deposition rate with increasing temperature indicated that the deposition was not a thermally-driven reaction. Using nitrous oxide slightly increased the nitrogen concentration in the film.

A mechanism of PECVD of SiO_2 film growth from organosilicon compounds, for instance, TEOS and oxygen feeds, was proposed by Fracassi

etc.. The proposed mechanism indicated that the overall deposition consisted of several concurrent heterogeneous and homogeneous reactions[52]: 1) precursor production in the plasma, which occurs for the reaction of TEOS with active species, oxygen atoms for instance; 2) adsorption on the substrate; 3) surface migration, which assures good step coverage; 4) reactions of the adsorbed radicals with the active species produced by the plasma, which decrease the carbon content of the film and lead to inorganic film precursors; 5) condensation of the inorganic radicals to form the SiO_2 network. The chemical structure of the precursors must be very close to that of TEOS, i.e., high organic carbon content, and therefore the fragmentation of the molecules must be kept low. Only in this case can the surface mobility of precursors be high enough to assure homogeneous surface concentration and therefore good step coverage.

This mechanism agreed with the experimental evidence, such as the effects of power density, substrate temperature, degree of ion bombardment, etc., and also explained the dependence of the step coverage on the deposition conditions[53-55].

1.4 New Precursors of SiO_2 Films

Various organosilicates have been used as chemical sources in place of silane not only for generating good quality SiO_2 films and optimizing the deposition conditions, but also for the safety purpose because silane is a toxic, pyrophoric

and potentially explosive gas. Some of these precursors are listed in Table 1.2.

Table 1.2 New Precursors of CVD SiO_2

Name	Formula	References
Tetraethoxysilane (TEOS)	$Si(OC_2H_5)_4$	9,22-25,29,30,37-42
Ethyltriethoxysilane (ETOS)	$C_2H_5Si(OC_2H_5)_3$	25-27,31
Amyltriethoxysilane	$C_5H_{11}Si(OC_2H_5)_3$	25,26
Vinyltriethoxysilane	$CH_2=CHSi(OC_2H_5)_3$	25,26
Phenyidiethoxysilane	$C_6H_5Si(OC_2H_5)_3$	25,26
Dimethyldiethoxysilane	$(CH_3)_2Si(OC_2H_5)_2$	25,26
Diphenyldiethoxysilane	$(C_6H_5)_2Si(OC_2H_5)_2$	25,26
Tetrapropoxysilane	$Si(OC_3H_7)_4$	28
Tetrabutoxysilane	$Si(OC_4H_9)_4$	28
Diacetoxyditertiary-butoxysilane(DADBS)	$(C_2H_5O)_2Si(OC_3H_7)_2$	30
Diethylsilane (DES)	$(C_2H_5)_2SiH_2$	14,27-29,31-35
Tetramethyicyclotetra-silane(TMCTS)	$Si_4(CH_3)_8$	35,36

Most of the work has been done with TEOS, using both LPCVD [9,22-25,29,30] and PECVD[37-42, 52-55] techniques. Optimum deposition conditions and their effects on the deposit properties have been studied in detail. A rough kinetic mechanism was proposed based on experimental results [52] (see section **1.3.3** for detail), though without unambiguous proof.

Diethylsilane(DES), the precursor used in this study, has a vapor pressure as high as 200mTorr at room temperature(25^{0}C). It can be processed into the reactor without the need of a carrier gas. Heating of the liquid source and the delivery line is not necessary either. The main properties of DES were listed in Table 1.3.

DES as a suitable chemical source for CVD SiO_2 film has been studied using LPCVD technique [27,28, 31-35,43,44]. Conformal films can be produced below 400^{0}C[27,35]. The deposition rate as a function of temperature was found to follow an Arrhenius behavior between 350-475^{0}C, yielding an apparent activation energy of 10 kcal/mol[31].

In PECVD processes, DES has been employed to synthesize silicon nitride[45]. The depositions were carried out over a temperature range of 100-300 ^{0}C, pressure range of 0.2-0.6 Torr, and the flow rate ratio of NH_3/DES varied from 6 to 26, rf power and frequency were kept at 0.15 W/cm^3 and 100 kHz. Under these conditions, the deposition rate was found to be proportional to the chamber pressure, and inversely proportional to the deposition temperature and NH_3/DES ratio.

Table 1.3 Properties of DES

Chemical name	diethyl silane (DES)
Chemical formula	$SiH_2 (C_2H_5)_2$
General Name	Organo-Hydro Silane
Molecular Weight	88.2
Appearance	Colorless liquid
Solubility in water	Insoluble
Autoignition Temperature	218 °C
Normal Boiling point	56 °C
Flash point	-20 °C (closed Cup)
Freezing Point	< - 76 °C (at 1 atm.)
Density	0.6843 g / cm^3 @ 20 °C
Vapor Density (air = 1)	> 1
Vapor pressure	207 Torr (@ 20 °C)

1.5 Objectives of This Thesis

Previous work on the PECVD of SiO_2 was focused on the film composition study, i.e., deposition parameters' effects on the film stoichiometry, impurities levels and so on. In this study, diethylsilane (DES) and nitrous oxide were used as the precursors of CVD SiO_2, using Plasma-enhanced CVD technique. The effects of

deposition parameters on the growth rate and physical properties of the PECVD SiO_2 films were investigated with comparison with the LPCVD SiO_2 films using DES as precursor and the PECVD processes based on silane and TEOS chemistry.

CHAPTER 2

EXPERIMENTAL

2.1 Set-up of the PECVD Apparatus

The synthesis of silicon dioxide films was carried out in the Applied Materials AMP 3300IIA PECVD system with an external DES flow control equipment. The scheme of the reactor is given in Figure 2.1. The reaction chamber is an aluminum cylinder with aluminum plates on both the top and the bottom, as upper electrode and susceptor, respectively. The diameter of the electrode and the susceptor are about 26 inches and the distance between the upper electrode and the susceptor is 2 inches. There are heater elements beneath the susceptor to heat it up.

Reactant gases were introduced into the reaction chamber separately before the rf power was supplied. The flow rate of nitrous oxide was controlled and measured by the built-in flow controller and can be obtained from the flow rate read-out and multiplied by the calibration factor of nitrous oxide vs. nitrogen, which was 0.71 (given by the manufacturer). DES flow was regulated by an automatic N_2 mass flow controller and was calibrated before the experiments.

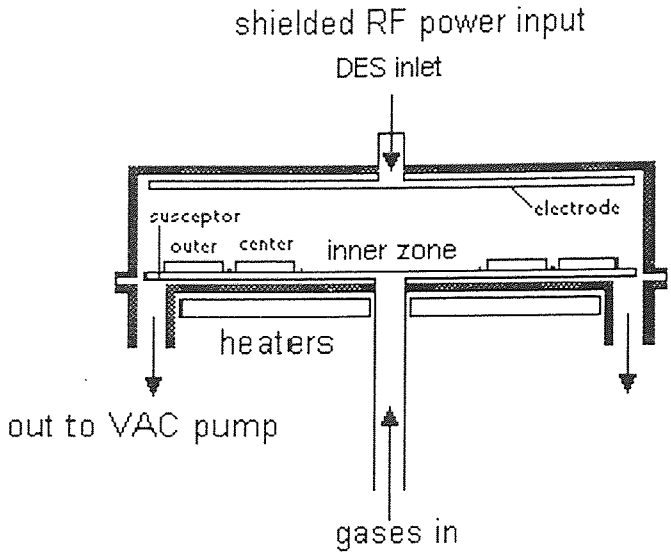

Figure 2.1 Schematic Diagram of PECVD Set-up

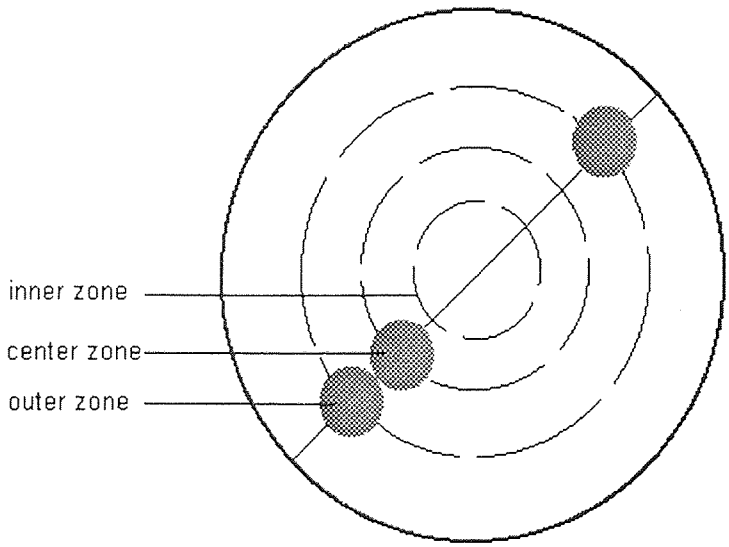

Figure 2.2 Schematic Diagram of the Susceptor

2.1 Pre-experiments

2.1.1 Susceptor Temperature Calibration

The temperature of the substrate is an essential parameter for deposition. But in the plasma reactor, there is no means to determine the absolute temperature under the deposition conditions. Therefore, susceptor temperature was used as a process variable. The susceptor which holds the substrate wafer is divided into three zones(Figure 2.1, Figure 2.2): inner zone, which has one heater element, center zone, which has three, and outer zone, which has two. Since the susceptor is heated through conduction of a metallic plate from the heater, there must be difference between the real susceptor temperature and the set point. So a temperature calibration was necessary before the experiments.

A J-type thermal couple was put in different position beneath the susceptor to monitor the temperature of each zone (see Figure 2.1, Figure 2.2). Measurement was done under the half-open-chamber condition. About one hour and a half was taken for the susceptor temperature to increase from one point to another and to become constant.

The temperatures of the outer zone and the inner zone were several degrees lower than those of the center zone, and the higher the temperature, the larger the difference. This can be attributed to the cooling effect of the surrounding air. (There is a gas inlet in the center of the susceptor). Thus it can be assumed that the temperature will be uniform when the chamber is

completely closed. It is more reasonable to take the temperature of the center zone as the susceptor(substrate) temperature.

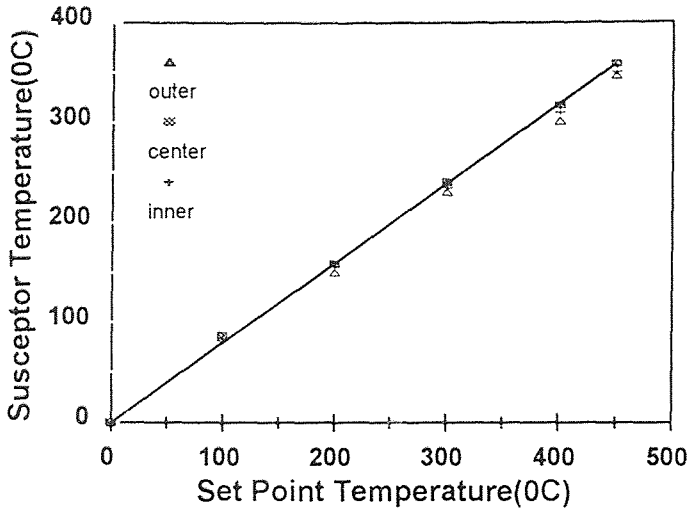

Figure 2.3 Temperature Calibration Curve

Figure 2.3 shows a linear relationship between the susceptor temperature and the set point. The function is:

$$Y = 0.7977\ X \qquad (2.1)$$

where Y is susceptor temperature (^{0}C);

X is set point temperature (^{0}C).

Then for the required substrate temperature of T (^{0}C), the heater should be set at 1.25T (^{0}C).

2.2.2 Flow Rate Calibration

An AFC automatic N_2 mass flow controller MFC (Applied Materials) was used to control and measure the DES flow rate.

The N_2 calibration of the MFC was checked by delivering a fix volume of gas (product of the metered flow rate and the time) into the known reaction chamber volume. The pressure increase was measured and used to calculate the volume of the gas corrected to the standard condition(0 ^{0}C, 1 atm). This process was repeated with DES to find out the correction factor. According to the gas law, the flow rate corrected to STP (sccm) is given by the formula below:

$$F.R. = 60(\Delta P/\Delta t)(T_0 V/P_0 T) \qquad (2.2)$$

where ΔP = pressure increase, Torr

T_0 = 273 K

P_0 = 760 Torr

V = volume of the chamber; cm^3

Δt = time of delivering gas, sec.

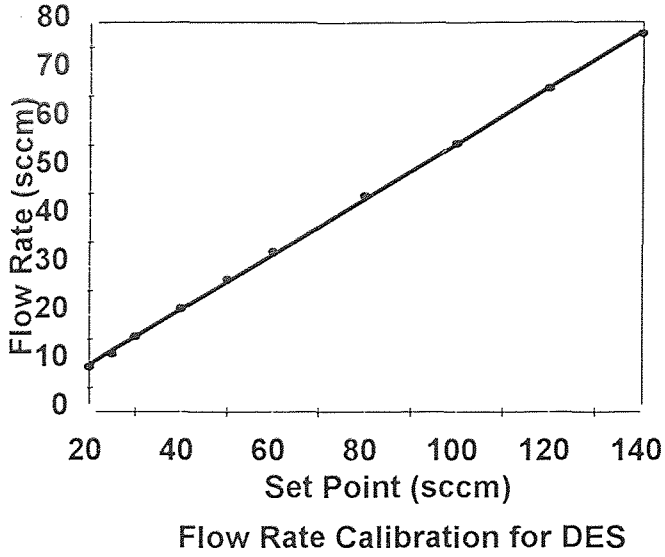

Figure 2.4 Flow Rate Calibration for DES

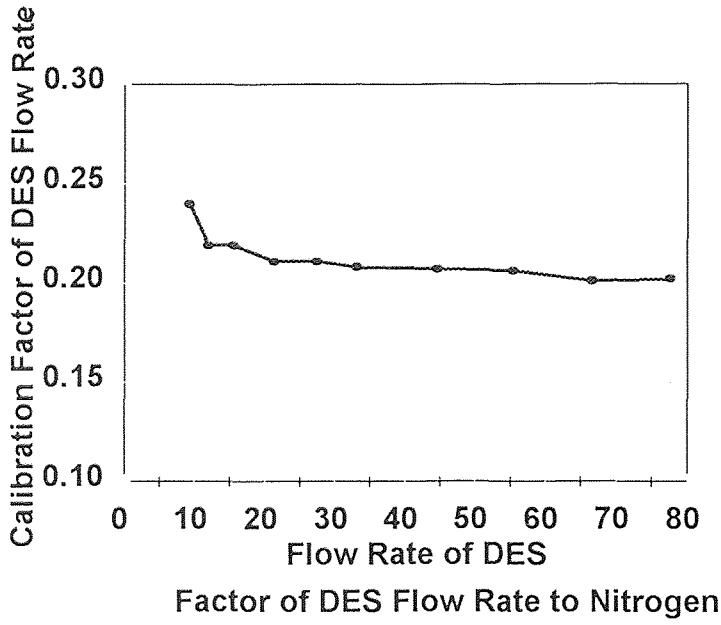

Figure 2.5 Flow Rate Calibration Factor of DES with Respect to Nitrogen

Figure 2.4 gives the calibration curve of DES flow rate, which was employed to obtain the actual flow rate of DES from the set point. The flow rate calibration factor which was taken as the flow rate ratio of DES to nitrogen is about 0.2 (Figure 2.5).

2.2.3 Leak Check

Routine leak checks were conducted everyday. After evacuating the chamber with valves and flow controller fully open, close the valves and calculate the leak rate from the chamber pressure rise. Typically the leakage is less than 6mTorr/min.

2.3 Experimental Procedures for Deposition

2.3.1 Wafer Loading

P-type single crystal silicon wafers, polished on one side, 10 cm in diameter, 525 um thick, marked and weighed with an accuracy of 0.1 mg, were placed horizontally on the susceptor. At the beginning, three wafers were mounted separately in the outer and center zones (see Figure 2.2). Those two placed in the symmetric position of the center zone are comparable, and the two along the radius are used to monitor the radical depletion effect. After the great depletion effect was observed, only two wafers were loaded in each run without the one posited in the outer zone.

2.3.2 Setting Deposition Conditions

After the substrates' loading, the reaction chamber and the reactant delivery lines were evacuated. The temperature controller was set to the desired point, and the susceptor was heated for an hour under the vacuum to ensure an uniform temperature. At the same time, the cooling water was turned on. The flow rate of DES and N_2O were set at their flow rate controllers respectively, and the total pressure, deposition time, plasma power and frequency were set at the engineering panel.

2.3.3 Film Deposition

When a constant temperature was reached, the deposition was started by pressing the START button in AUTO state, DEPOSITION MODE. The chamber was pumped down to the base pressure. The sequential steps included: high purging, prepurging and processing gas (with the indicator lights on). The DES flow controller was opened manually since it was not controlled by the machine. The gases were processed into the reaction chamber at the set flow rate automatically controlled by the system. The total pressure was also adjusted to the set value automatically at the PROCESS GASES stage. After the flow rate of reactant gases and the system pressure were maintained at the desired level, the rf power was applied and the deposition started.

2.3.4 Post-deposition Procedure

When the deposition was advanced to the set time, the rf power would shut off automatically. The chamber was pumped down and cooled down under the vacuum to below 100^0C with the cooling water on to avoid any undesired reactions. The chamber was back-filled with nitrogen, the wafers were then taken out and weighed. As soon as the wafers were removed, the chamber was evacuated and kept under vacuum. The deposit properties were then determined by the characterization techniques.

2.2.4 Reactor Etching

During the deposition reactions, films also have been deposited on the upper electrode and the susceptor. The reactor must be cleaned in order to remove the deposits in the reactor chamber, which may peel and affect the deposition process. As suggested by the Applied Materials AMP-3300IIA PECVD system user's manual, the chamber was etched after every 5 microns(50,000Å) deposit, and the etching are performed under the following conditions for 45 minutes: chamber pressure = 0.3 Torr, oxygen flow rate = 200 sccm, Freon flow rate = 300 sccm, plasma power = 800 W (power density = 0.24 W/cm^2), with the heater off (typically about 100 ^{0}C).

2.4 Characterization of SiO_2 Thin Films

2.4.1 Thickness

Film thickness was measured by Nanospec Interferometer which bases its estimation on the monochromatic light interface fringes formed within a zone limited by the sample surface and a semi-transparent mirror. The device consists of Nanometrics NanoSpec/AFT microarea gauge and SDP-2000T film thickness computer. The thickness of the film deposited on the wafer was measured at five different points, as shown in Figure 2.6. The refractive indexes provided were first estimated, as for silicon dioxide thin film, 1.46 is the typical value, then used the real value measured by the ellipsometer (see section **2.4.2**). The average value was taken as the film thickness. Uniformity in radial distribution of the deposits was estimated from the relationship: $(T_{max} - T_{min})/(T_{max} + T_{min}) \times 100$.

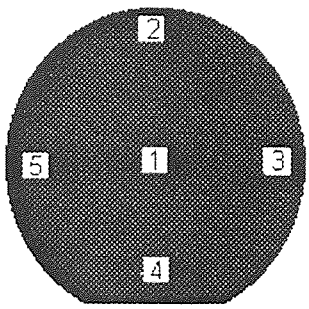

Figure 2.6 Wafer Image Showing the Points of Thickness Measurement

Deposition rate was determined as the film thickness over the deposition time , i.e., $D.R. = \Delta T/\Delta t$, and averaged over the two wafers in the center zone deposited in each run.

Film density was estimated from the mass-volume relationship. Since the wafer area is known to be 78.5 cm^2 and deposition occurred only on one side, the density can be calculated from the mass increase of the wafer due to film formation and the average thickness of the film.

2.4.2 Refractive Index

The refractive index of the deposits was determined by a Rudolph Research AutoEL ellipsometer, which consists of a polarizer and a compensator. Plane (45^0) polarized light from the polarizer is elliptically polarized when it passes through the compensator. It is then reflected by the sample surface, collected by a detector, analyzed for its intensity and finally quantified by a set of delta psi values. The values were then fed to a computer which numerically solves the equation to give the refractive index of the film.

2.4.3 Infrared Spectra

Infrared spectroscopic analysis was done on a Perkin-Elmer 1600 Series FTIR spectrophotometer to determine the characteristics of the deposits. The 1080 cm^{-1} absorption band arisen from the vibration of Si-O-Si was used for quantitative analysis of silicon dioxide. The shifting of this band indicates the

dense change of the silicon dioxide[46, 47], i.e., higher frequency is contributed by more dense and large Si-O-Si bond angle than lower frequency. Other absorption bands at 800 cm^{-1} and 460 cm^{-1} indicate the in-plane bending and out-of -plane rocking vibration of Si-O-Si respectively. The absorptions at 1080, 800 and 460 cm^{-1} are characteristic of SiO_2. the two absorptions at 3620 and 3380 cm^{-1} are O-H stretching mode caused by loosely bonded SiOH or H_2O. The 2270 cm^{-1} absorption is a Si-H stretch. The 880 cm^{-1} and has been assigned to Si-H, Si-H or nonbridging oxygen[37].

2.4.4 Stress

The stress of the film was determined by a house-developed device, employing a laser-beam equipment which measures change in the radius of curvature of the wafer resulting from the film deposited on one side. Two fixed and parallel He-Ne laser beams were incident on the wafer surface before and after deposition. The reflected beams from the two surfaces was then projected by an angled plane mirror as two points onto a scale in a certain distance thus their separation could be measured more accurately. The change in the separation of these two points was then fed into Stony's Equation[6] to obtain actual stress value. The calculation formula is:

$$\delta = 12.3D/T \qquad (2.3)$$

Where D = distance difference between the two image points before and after the deposition (mm);

T = thickness of the film (μm);

δ = stress of the film (MPa), negative value indicates compressive stress.

2.4.5 Etch Rate

P-etch process was selected to measure the etch rate of the PECVD SiO_2 film. P-etch solution consists of 15 parts HF (49%), 10 parts HNO_3 (70%) and 300 parts distilled water.

A piece of the wafer was immersed in P-etch solution at room temperature (about 25 ^{0}C) for 30 seconds, then the thickness of the remained film was measured. The etch rate of the film was obtained from the slope of the linear plot of thickness versus etching time.

2.4.6 Hardness and Young's Modulus

The hardness and Young's modulus of the films were determined using a Nano Instruments indenter. The system consists of a pyramid-shaped diamond tip, with the same area to depth ratio as the traditional Vickers pyramid, mounted on a loading column that is suspended on thin leaf springs. At the top of the loading column is a coil and magnet assembly that provides a controlled loading force towards the sample with a resolution of about 0.5 μN. The force imposed on the column is controlled by varying the current in the coil. The position of the

indenter is determined by a capacitance displacement gauge which detects displacement changes of 0.2-0.3 nm. A plot of load (mN) versus displacement (nm) can be obtained and the hardness and Young's modulus obtained.

CHAPTER 3

RESULTS AND DISCUSSIONS

3.1 Depletion Effect

Figure 3.1 shows the depletion effect of gas flow along the radius of the susceptor. When the total flow rate was 135 sccm, the deposition rate of the wafer which was positioned in the outer zone was less than 50% of that in the center zone. So it is not recommended to put wafers in the outer zone. Following experiments were done only in the center zone.

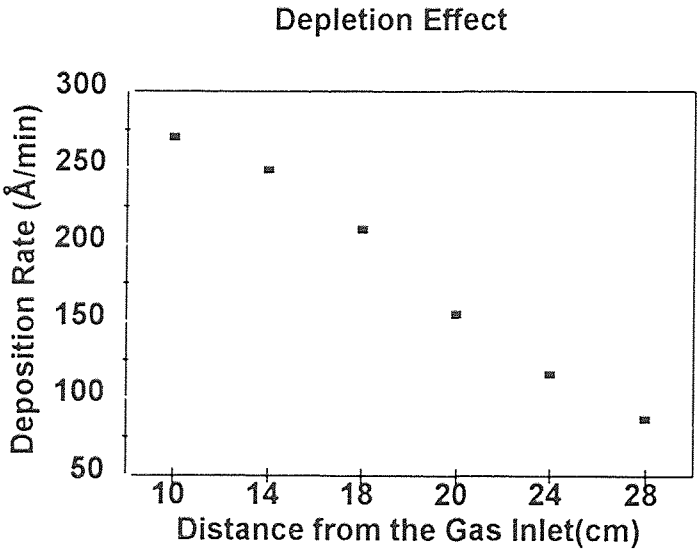

Figure 3.1 Radical Depletion Effect at Deposition Condition 300 ^{0}C, 300 mTorr, Flow Rate N_2O=120 sccm, DES=15 sccm, Plasma Power 0.15W/cm^2 100kHz

3.2 Temperature Effect

Temperature effect on the growth rate and properties of the SiO_2 films was studied over a series of temperatures ranging from 100 ^{0}C to 350 ^{0}C. The flow rates of DES and nitrous oxide were set at 15 sccm and 120 sccm, respectively. Total pressure of the reactor was maintained at 0.3 Torr. Plasma power was kept at a constant level of 500 W (0.15 W/cm^2) and frequency was fixed at 100 kHz throughout the temperature series study.

In the range studied, the growth rate decreased from 794 Å/min to 213Å/min as the susceptor temperature increased over an interval of 250 ^{0}C, as shown in Figure 3.2.

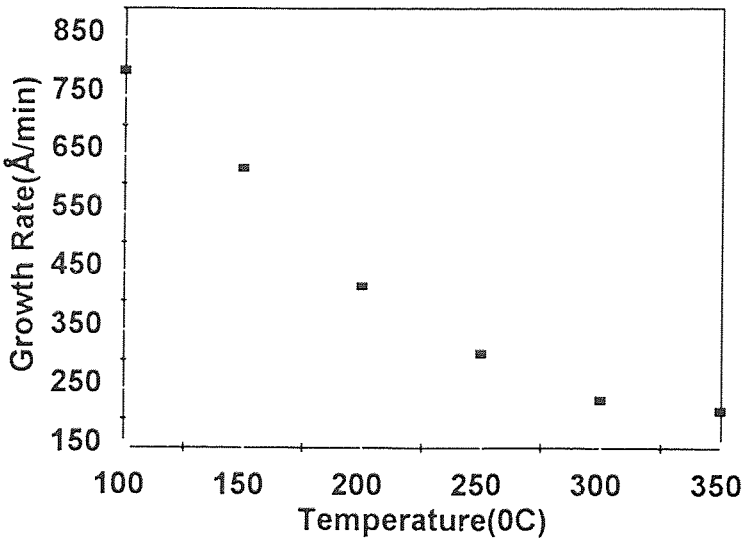

Figure 3.2 Variation of Growth Rate as a Function of Temperature at Fixed Flow Rate Ratio N_2O/DES = 8:1, Pressure = 300 mTorr, Plasma Power Density = 0.15 W/cm^2, rf = 100 kHz

The decrease in growth rate with increasing temperature were also observed in the PECVD process of silicon dioxide from silane[50] and TEOS[38] and PECVD process of silicon nitride from DES[45], which was contrary to the temperature dependence of LPCVD processes.

The difference maybe attributed to the different roles of thermal energy played in these two kinds of reactions. Surface reaction included thermal decomposition of the reactant gas molecules, was the rate-controlling step of LPCVD process. Thus growth rate generally increases with increasing temperature. The reactions followed the Arrhenius behaviors. Arrhenius plot was obtained in certain temperature range[31,38]. While the PECVD processes were driven by the free radicals which are produced primarily by electron impact dissociation, for instance, oxygen radical O* and SiH_2* in this study, elevated temperature increased the collision of reactive radicals which causing gas phase nucleation and the opportunities of the O* recombination to O_2[56], which in turn reduced the probability of the deposition reaction occurring.

Figure 3.3 shows the film density increased with increasing temperature and the values are lower than the thermally grown oxide, which was 2.27g/cm^3. This may be attributed to the loose structure of the amorphous deposit and the moisture and/or product gases trapped in the porous film. The lower the temperature, the higher the growth rate, the looser structure of the film, the larger tendency of absorbing those impurities. Decrease of P-etch rate with the

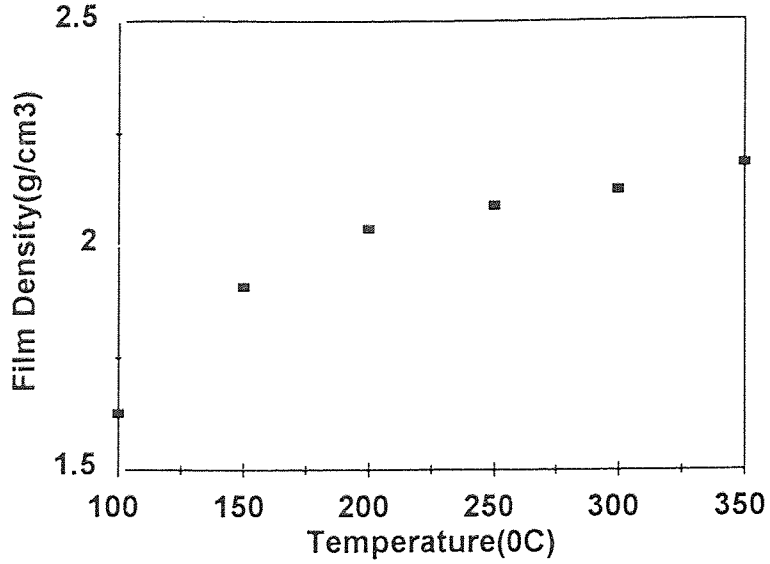

Figure 3.3 Variation of Film Density as a Function of Temperature at Fixed Flow Rate Ratio N_2O/DES = 8:1, Pressure = 300 mTorr, Plasma Power Density = 0.15 W/cm^2, rf = 100 kHz

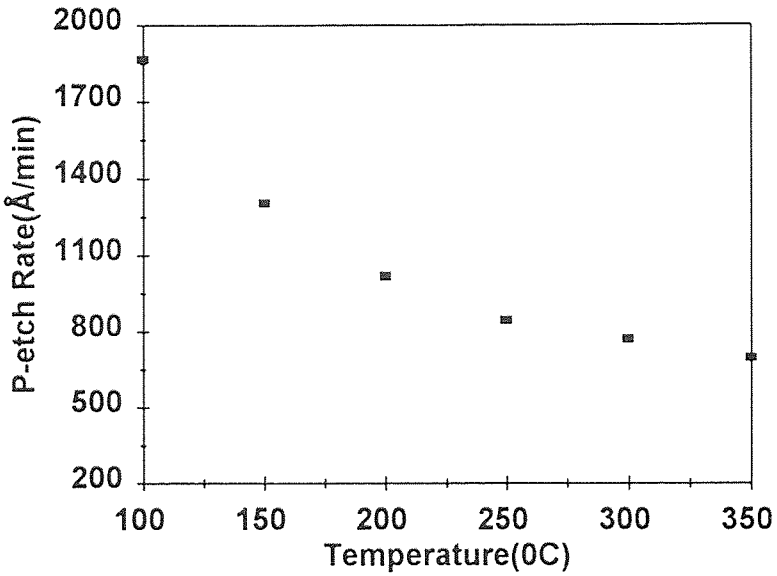

Figure 3.4 Variation of P-etch Rate as a Function of Temperature at Fixed Flow Rate Ratio N_2O/DES = 8:1, Pressure = 300 mTorr, Plasma Power Density = 0.15 W/cm^2, Rf = 100 kHz

increasing temperature (see Figure 3.4) was in good agreement to the density variation, which strongly supported the above explanation.

The measurements of film hardness and Young's modulus gave consistent trend with density(Figure 3.5, Figure 3.6). The higher the temperature, the denser the film, the higher values of hardness and Young's modulus.

The stress of the films was compressive at all temperatures, the same as other PECVD films, and decreased with increasing temperature (Figure 3.7). It can be said that the compressive stress increased with increasing film density.

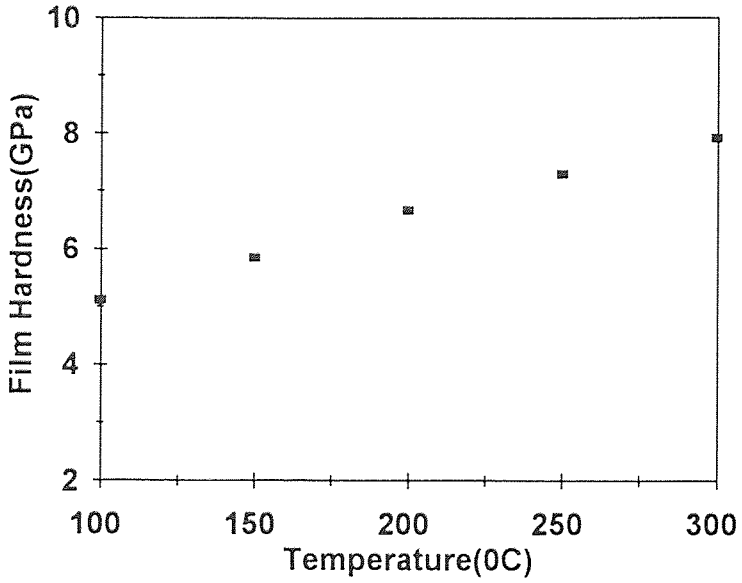

Figure 3.5 Variation of Hardness as a Function of Temperature at Fixed Flow Rate Ratio N_2O/DES = 8:1, Pressure = 300 mTorr, Plasma Power Density = 0.15 W/cm^2, Rf = 100 kHz

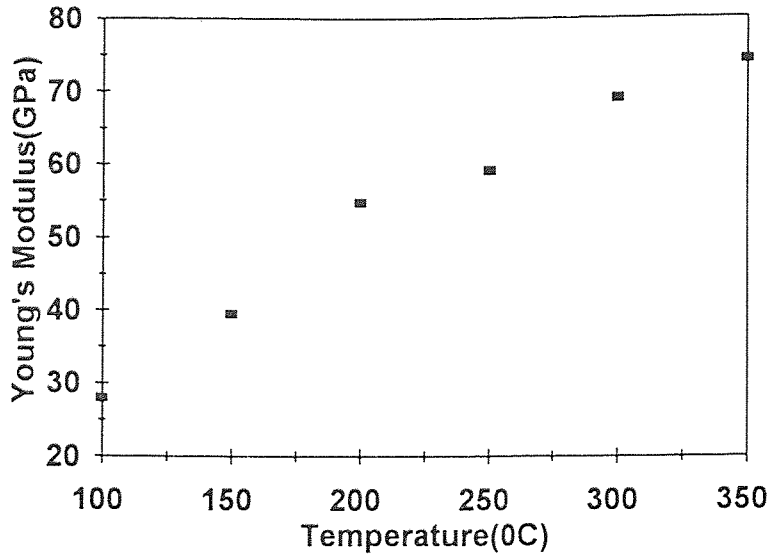

Figure 3.6 Variation of Young's Modulus as a Function of Temperature at Fixed Flow Rate Ratio N_2O/DES = 8:1, Pressure=300mTorr, Plasma Power Density = 0.15 W/cm^2, Rf = 100 kHz

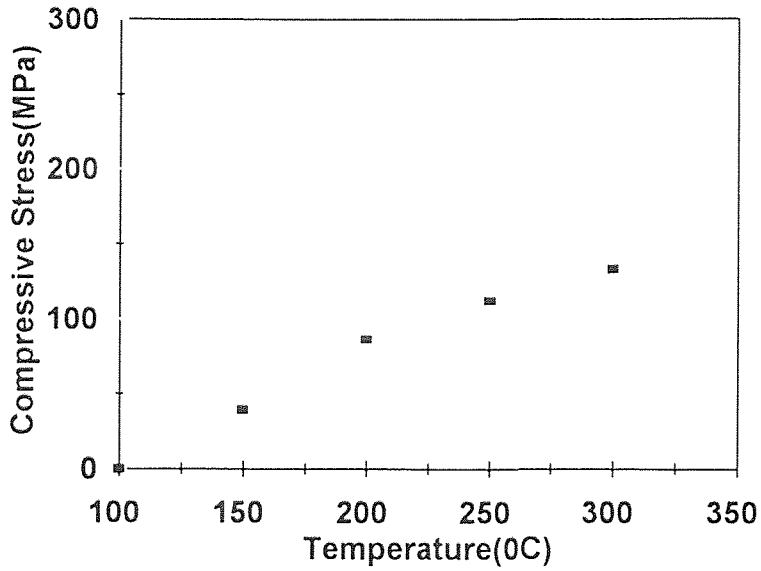

Figure 3.7 Variation of Film Stress as a Function of Temperature at Fixed Flow Rate Ratio N_2O/DES = 8:1, Pressure = 300 mTorr, Plasma Power Density = 0.15 W/cm^2, Rf = 100 kHz

The refractive index of the deposits is higher than the thermal oxide which is 1.46 (Figure 3.8). This may be caused by the oxygen-deficient films which were generally observed in PECVD oxides[38,50], and/or more polar impurities such as water molecules and hydroxyl groups of the silanol[51] as well as carbon impurities.

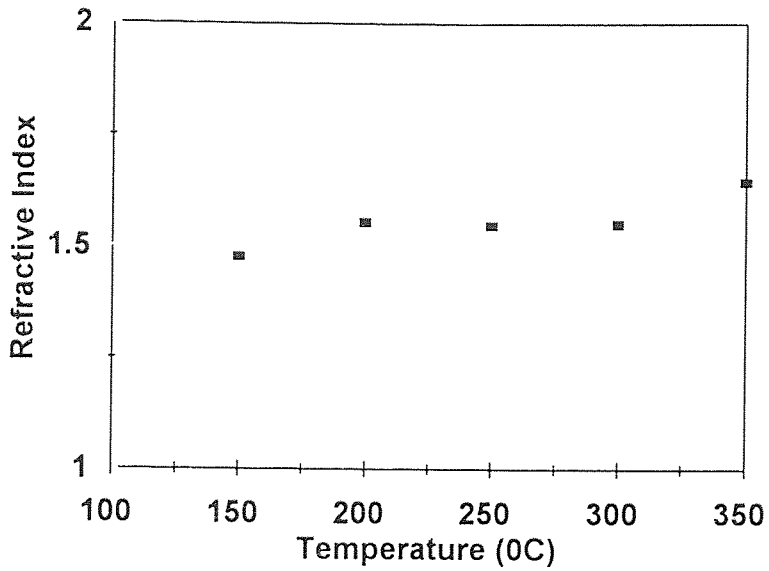

Figure 3.8 Variation of Refractive Index as a Function of Temperature at Fixed Flow Rate Ratio N_2O/ DES=8:1, Pressure=300mTorr, Plasma Power Density = 0.15 W/cm^2, Rf = 100 kHz

In Figure 3.9, a typical FTIR spectrum of the PECVD SiO_2 film deposited from DES and N_2O under the experimental conditions is given. The three absorptions at 1080cm^{-1}, 800cm^{-1}, 460 cm^{-1} characterized SiO_2. Very little shift of the 1080 cm^{-1} peak with changing temperature was observed. The broad absorption at about 3600 cm^{-1} which was assigned to O-H stretching[37] can be

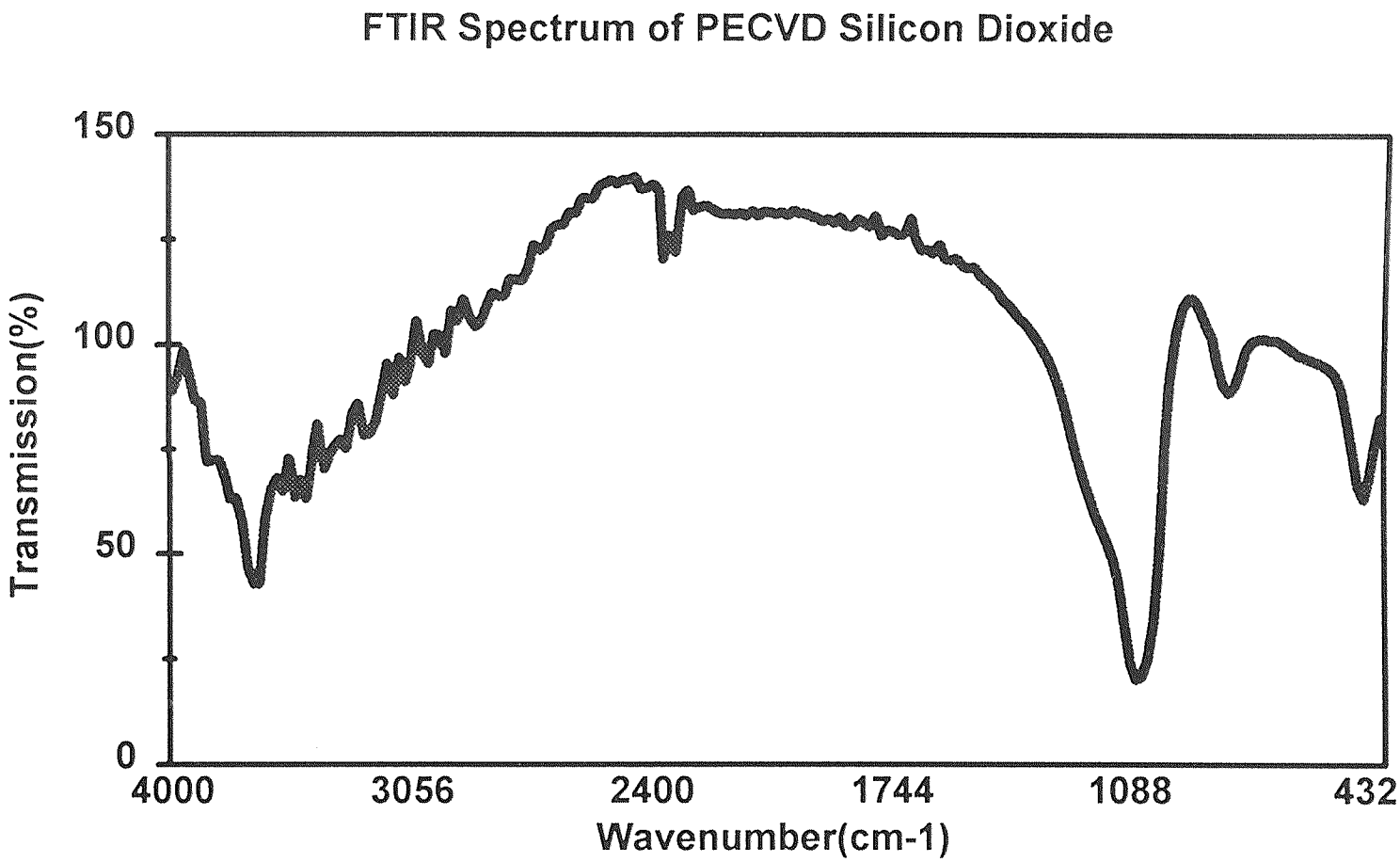

Figure3.9 Typical FTIR Spectrum of PECVD Silicon Dioxide

attributed to the moisture trapped in the film or loosely bonded SiOH. The small absorption peak("shoulder")at 880 cm^{-1} was also due to this silanol bond. Unlike other work[31], no trend of the intensity of this 880 cm^{-1} peak associated with temperature variation was observed. The peak of 2270 cm^{-1} was characteristic of CO_2, which might be in the air of the chamber.

Within the framework of temperature window investigated, 300^0C appeared to be a plausible temperature that could yield quality oxide deposit at a moderated growth rate. Therefore, further studies were carried out at the fixed temperature 300^0C.

3.3 Gas Composition Study

The gas composition study was carried out with invariant temperature (300 ^{0}C), pressure (300 mTorr), DES flow rate (15 sccm) plasma power (500 W/cm^2), and rf frequency (100 kHz). Thus, the total flow rate of the reactant gases increases with the increase of N_2O/DES flow rate ratio.

Figure 3.10 shows the growth rate increased with the increasing N_2O/DES ratio in the range 8-20, i.e., total flow rate from 135 to 315 sccm (Figure 3.11). While in the low ratio range, N_2O/DES ratio were 2-4, total flow rate were 45-95 sccm, the growth rate decreased as the flow rate ratio and total flow rate increased. It appeared to be principally a densification process in this range. There was a little change in the mass of the deposits. The low growth rate resulted from a higher density film (Figure 3.12) with its corresponding low etch

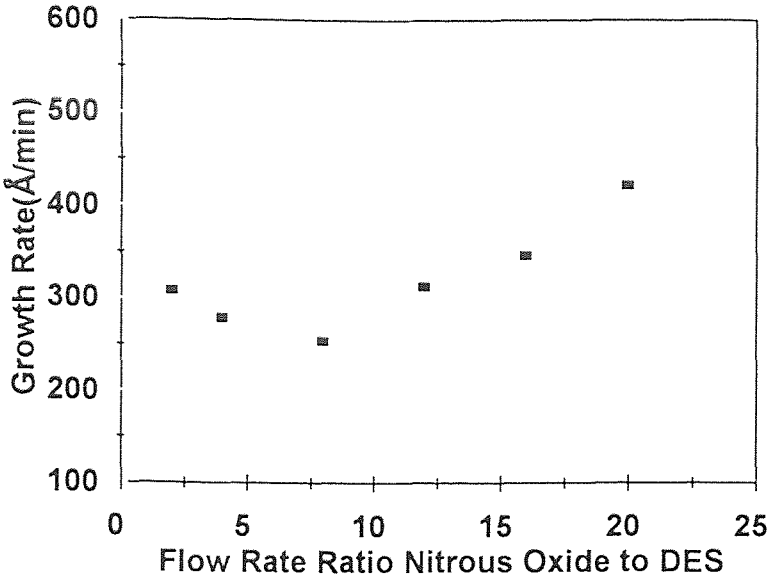

Figure 3.10 Variation of Growth Rate as a Function of Flow Rate Ratio at Fixed Temperature 300°C, Pressure = 300 mTorr, Plasma Power Density 0.15W/cm^2, rf 100 kHz

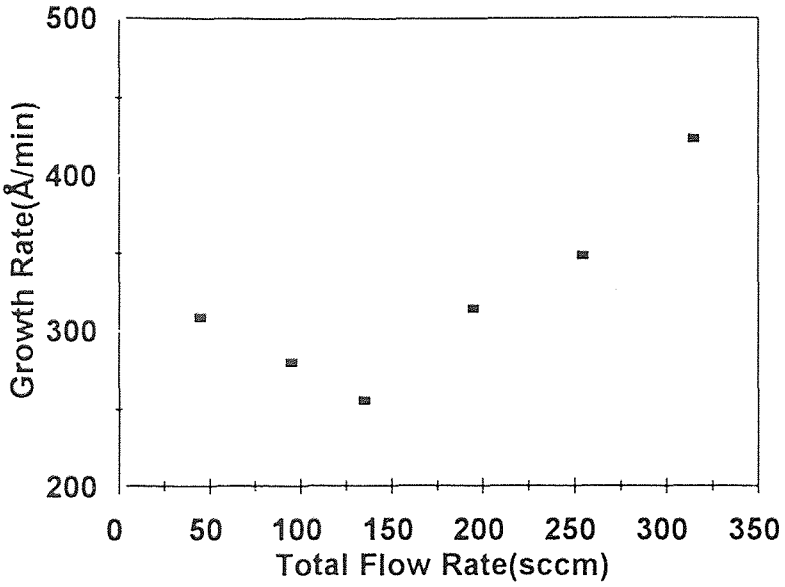

Figure 3.11 Variation of Growth Rate as a Function of Total Flow Rate at Fixed Temperature 300°C, Pressure = 300 mTorr, Plasma Power Density 0.15W/cm^2, rf 100 kHz

rate (Figure 3.13). In the high ratio range (>8), film density slightly decreased with the relatively large increase in growth rate. The increase of mass with total flow rate (Figure 3.14) proved the "real" increase in deposits as the total flow rate increased. A possible explanation for this phenomena may be that, the flow rate was too low to remove the product gas molecules when it was lower than 135 sccm, thus films deposited under such conditions might trapped more gas molecules, showing high growth rate but low density and high etch rate. As the total flow rate as well as the N_2O flow rate became high enough, no further densification occurred. Growth rate increased but density almost did not change. There might be two factors responsible for the significant increase in the growth rate. One was the increasing amount of the oxygen radical O* available in the plasma, which dominated the plasma oxidation reaction, accelerated the deposition. The other lay in the increasing reactant gases feed and increasing products removal, which favored the deposition reactions. Under these circumstances, both mass increasing rate (mg/min) and growth rate(Å/min) increased with the increasing flow rate while the film density almost unchanged. The etch rate did not change either (Figure 3.15), consistent with the density trend.

The variation of refractive index showed a consistent trend with the density change (Figure 3.15), i.e., lower density films showed higher refractive index, indicating more polar molecules (such as water, silanol, etc.) in the deposits, which also resulted in the decrease of the film density. Moisture

existence was proved in FTIR spectra(see Figure 3.9). No Si-C bond stretching or vibration mode was indicated in the FTIR spectra.

Hardness and Young's modulus varied with the density (Figure 3.16, Figure 3.17) too. Denser film had higher hardness and Young's Modulus. Both gave further evidence of the densification process.

Film stress seemed to be independent upon the gas composition, showing no trend with the varying flow rate (Figure 3.18).

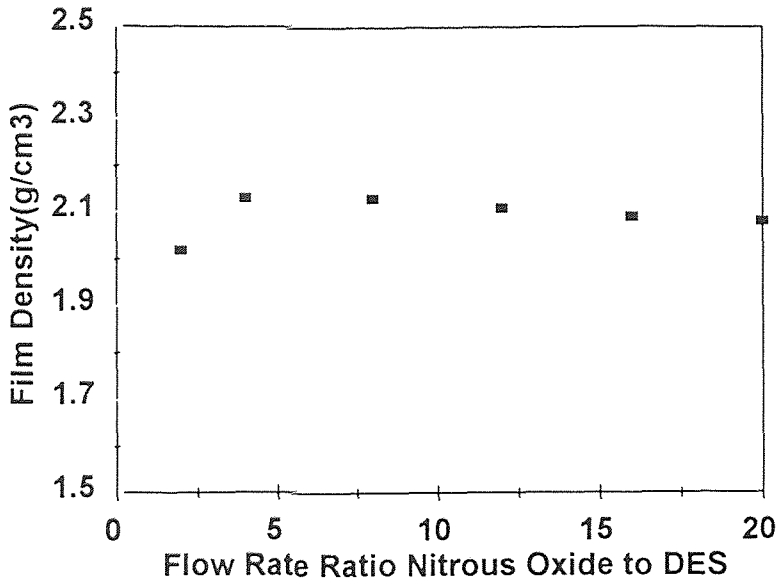

Figure 3.12 Variation of Film Density as a Function of Flow Rate Ratio at Fixed Temperature 300^{0}C, Pressure = 300 mTorr, Plasma Power Density 0.15W/cm^2, rf = 100 kHz

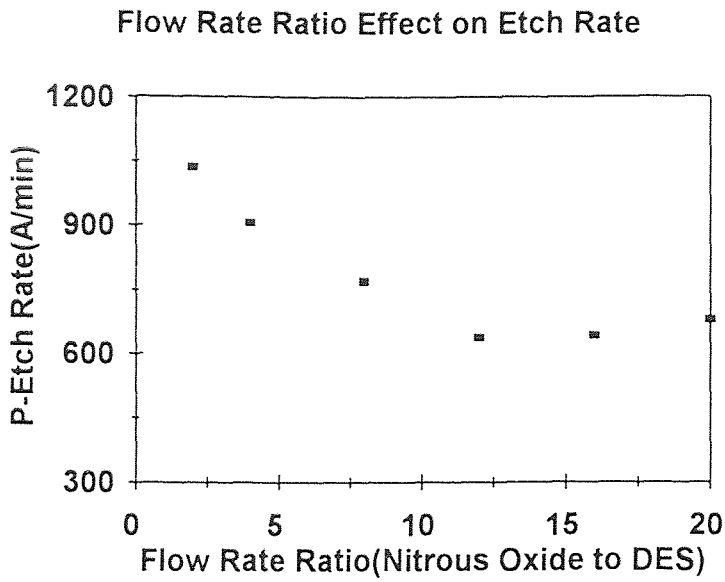

Figure 3.13 Variation of P-etch Rate as a Function of Flow Rate Ratio at Fixed Temperature 300°C, Pressure = 300 mTorr, Plasma Power Density 0.15W/cm^2, Rf = 100 kHz

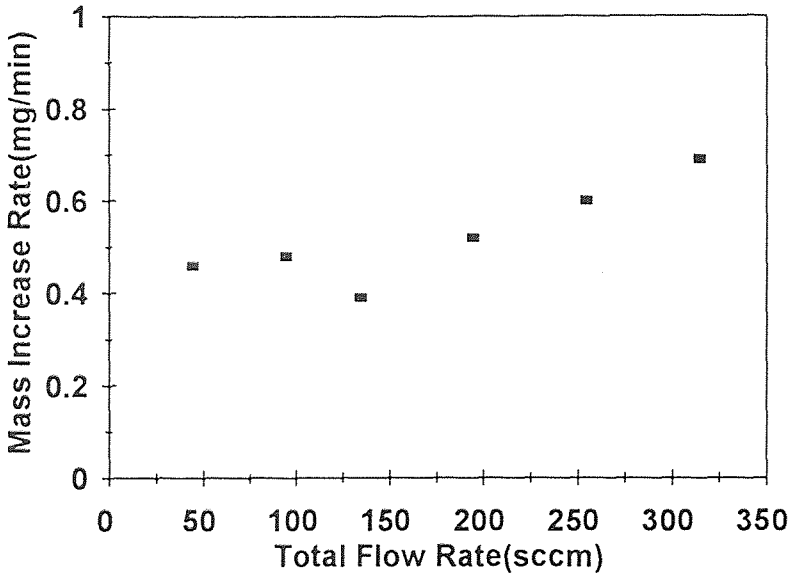

Figure 3.14 Variation of Mass Increase Rate as a Function of Total Flow Rate at Temperature 300°C, Pressure = 300 mTorr, Plasma Power Density 0.15W/cm^2, rf = 100 kHz

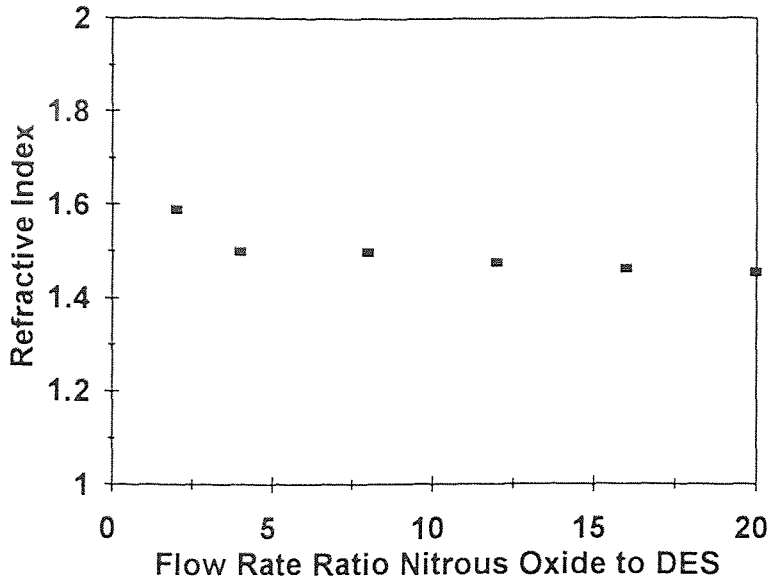

Figure 3.15 Variation of Refractive Index as a Function of Flow Rate Ratio at Temperature 300^{0}C, Pressure = 300 mTorr, Plasma Power Density 0.15W/cm^2, rf = 100 kHz

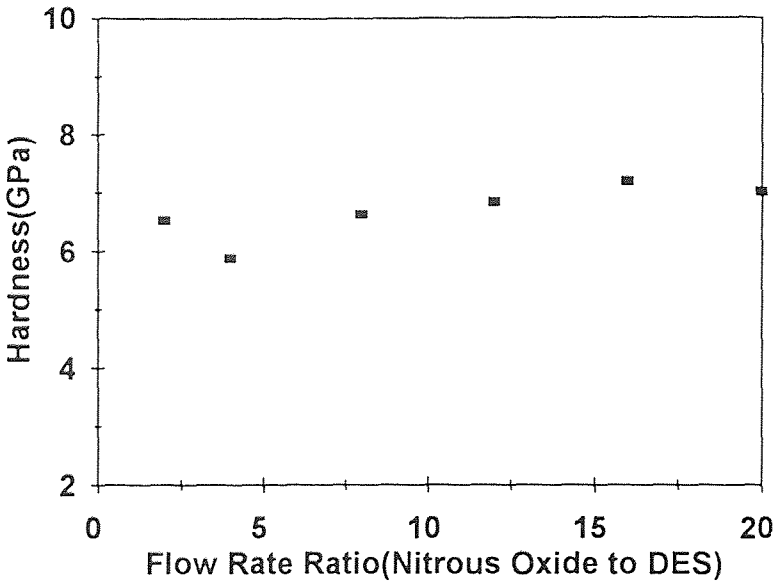

Figure 3.16 Variation of Hardness as a Function of Flow Rate Ratio at Fixed Temperature 300^{0}C, Pressure=300mTorr, Plasma Power Density 0.15W/cm^2, Rf = 100 kHz

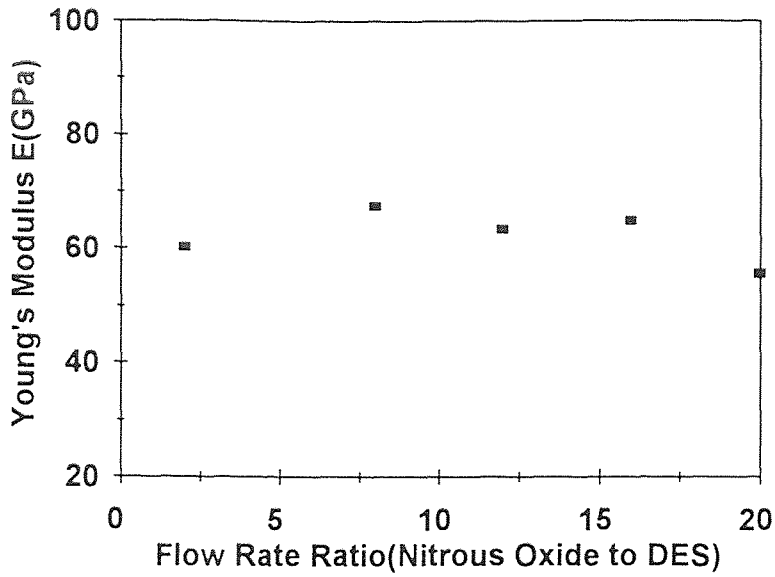

Figure 3.17 Variation of Young's Modulus as a Function of Flow Rate Ratio at Temperature 300^{0}C, Pressure = 300 mTorr, Plasma Power Density 0.15W/cm^{2}, Rf = 100 kHz

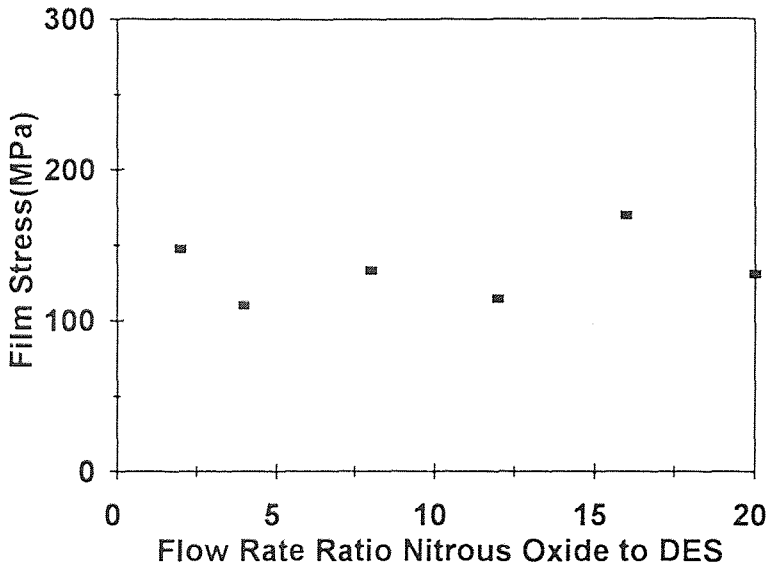

Figure 3.18 Variation of Film Stress as a Function of Flow Rate Ratio at Fixed Temperature 300^{0}C, Pressure = 300 mTorr, Plasma Power Density 0.15W/cm^{2}, Rf = 100 kHz

Changes in film composition or stoichiometry were expected with the variation of the feeding gas composition. But the FTIR spectra were almost the same as shown in Figure 3.9, no obvious change was found.

Based on this series study, N_2O/DES = 16:1 appeared to be an optimized flow rate ratio, resulting in a high growth rate (327 Å/min), high density (2.14g/cm^3) and other good qualities. Further studies were performed at this ratio, i.e., N_2O flow rate = 240 sccm, DES flow rate = 15 sccm.

3.4 Pressure Effect

Pressure study was carried out at 300^{0}C over a pressure range of 150 mTorr to 700 mTorr with constant flow rate of N_2O = 240 sccm, DES = 15 sccm. Plasma power and rf frequency were also kept at 500 W (0.15 W/cm^2) and 100 kHz , respectively.

In previous work, the growth rate of PECVD films was found to decrease with increasing pressure as a result of gas phase reaction[51, 56]. However, under the conditions studied here, it behaved as shown in Figure 3.18. The growth rate increased as the pressure increased from 150 mTorr to 500 mTorr, and then saturated at the high pressure range 500-700 mTorr. A similar pressure dependence except for the plateau was obtained by Y. Yu[45] in the PECVD of silicon nitride.

From Figure 3.20, it can be seen that the density was almost constant as

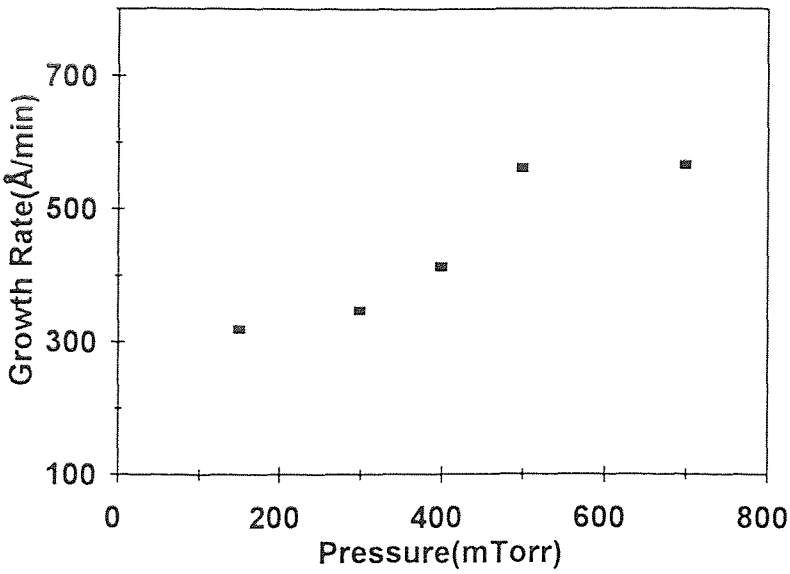

Figure 3.19 Variation of Growth Rate as a Function of Pressure at Temperature 300^{0}C, Flow Rate Ratio N_2O/DES = 16:1, Plasma Power Density 0.15W/cm^2, rf 100 kHz

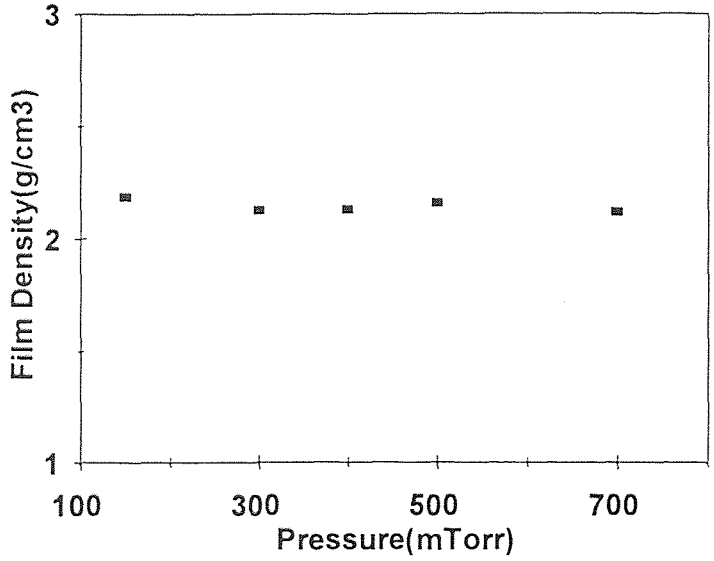

Figure 3.20 Variation of Film Density as a Function of Pressure at Temperature 300^{0}C, Flow Rate Ratio N_2O/DES = 16/1, Plasma Power Density 0.15W/cm^2, rf 100 kHz

the growth rate increased. However, the P-etch rate increased with the increasing pressure and growth rate (Figure 3.21). The films with high etch rate displayed a corresponding low low value for hardness and Young's modulus (Figure 3.23, Figure 3.24).

High pressure is resulted from more gas molecules in the chamber for a longer time. In the plasma field, the longer the gas molecules stay, the larger amount of radicals and ions will be produced . Higher concentration of these reactive species on one hand enhanced deposition reaction and thus resulted in higher growth rate without a decrease in density, on the other hand, it led to more ion bombardment towards the substrate surfaces and caused more defects

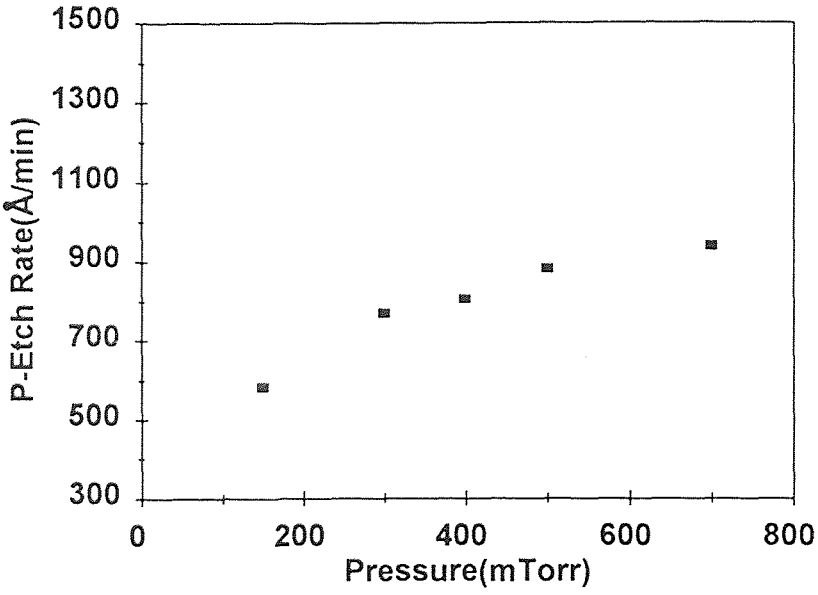

Figure 3.21 Variation of P-etch Rate as a Function of Pressure at Temperature 300^{0}C, Flow Rate Ratio N_2O/DES = 16/1, Plasma Power Density 0.15W/cm^2, rf 100 kHz

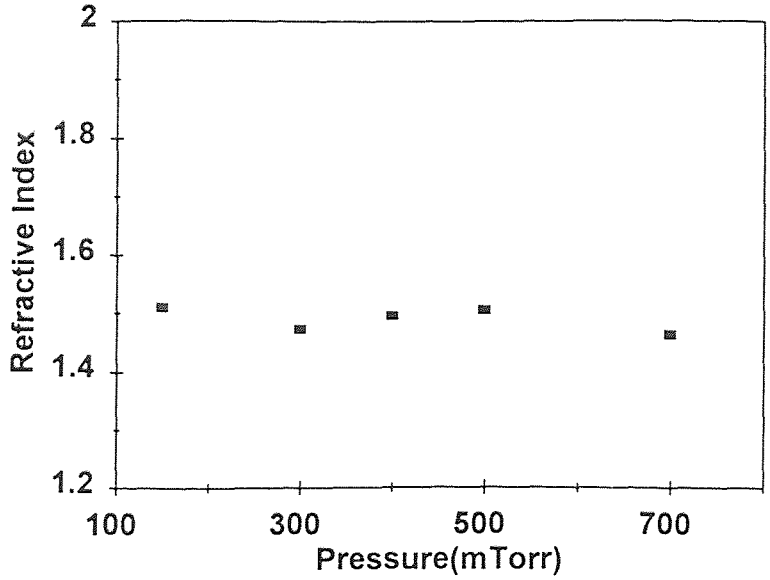

Figure 3.22 Variation of Refractive Index as a Function of Pressure at 300^{0}C, Flow Rate Ratio N_2O/DES = 16/1, Power Density 0.15 W/cm^2, rf 100 kHz

in the deposited films. Difficulty in getting reliable refractive index (see Figure 3.22) can be taken as an indirect proof of high defects concentration. Therefore, high pressure tended to result in poor quality films with high etch rate, low hardness and Young's modulus at high growth rate.

Because the plasma power is fixed, at a certain pressure, an equilibrium between ionization caused by electron impact and ion recombination was reached. The ion concentration did not increased as the number of gas molecules increased, but reached the maximum value. Consequently, further increase in growth rate did not occur and film properties, including P-etch rate, hardness and Young's modulus, were unchanged, as shown in Figure 3.19, 3.21, 3.23, and 3.24.

The film deposited at 150 mTorr showed a high growth rate and good properties such as high density, low P-etch rate, high hardness and Young's modulus. However, its refractive index was higher than the typical values of CVD SiO_2 and what were mostly obtained in this study. Impurity levels, most likely carbon contents might be high, though neither new peaks nor significant change in the FTIR spectra was observed. Film composition analysis was needed to give further evidence.

Thus, pressure = 300 mTorr along with temperature = 300 ^{0}C, flow rate of N_2O = 240 sccm, DES = 15 sccm, power density = 0.15 W/cm^2 and rf = 100 kHz was still considered as an optimized deposition condition.

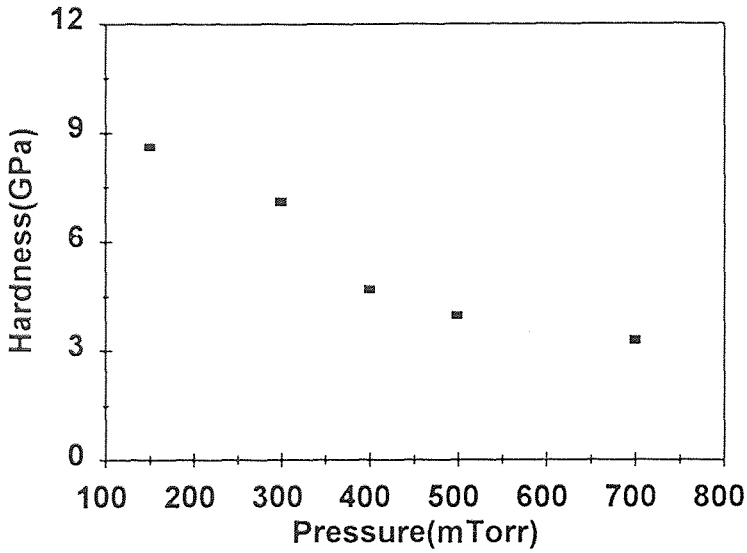

Figure 3.23 Variation of Hardness as a Function of Pressure at 300^{0}C, Flow Rate Ratio N_2O/DES = 16/1, Power Density 0.15W/cm^2, rf 100 kHz

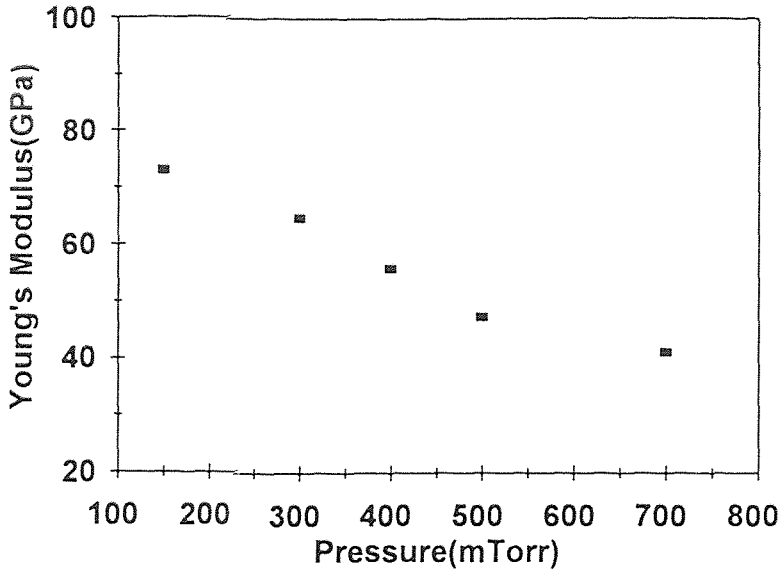

Figure 3.24 Variation of Young's Modulus as a Function of Pressure at 300^{0}C, Flow Rate Ratio N_2O/DES = 16/1, Power Density 0.15 W/cm^2, rf 100 kHz

CHAPTER 4

CONCLUSIONS

Silicon dioxide thin films were deposited on silicon wafers by Plasma-Enhanced Chemical Vapor Deposition (PECVD) using diethylsilane(DES) as a precursor and nitrous oxide as the oxidant. The effects of process such parameters as susceptor temperature, gas composition, and reactor chamber pressure on the deposition and film properties were investigated. The films were characterized by measuring growth rate, density, P-etch rate, refractive index, stress and infrared spectra.The growth rate was found to be inversely proportional to the temperature in the range 100-300 ^{0}C. It increased with the flow rate ratio of N_2O/DES as the total flow rate fell into 135 sccm-315 sccm. It also increased with the pressure and reached saturation.

Within the framework of these variables study, quality silicon dioxide thin films were obtained at 300 ^{0}C, 300 mTorr, nitrous oxide flow rate 240 sccm, DES flow rate 15 sccm under 500 W,100 KHz plasma power with high growth rate as 327 A/min. The resulted deposits were amorphous, moisture containing, with a density of 2.14g/cm^3, refractive index 1.474, P-etch rate 632 Å/min and compressive stress.

REFERENCES

1. Coulson, A. R.; Tauber, R. N.,In *Silicon Processing for the VLSI ERA;* Wolf, R., Tauber, R. N., Eds.; Lattice Press: Sunset Beach, California,1987

2. Riedling, K., *Ellipsometry for Industrial Applications,* Springer-Verlag/Wien: New York,1988

3. Ramos , E.; Datta, A.; Levy,R.A.; Krasnoperov, L. N.; Grow, J. M.; *Synthesis of Silicon Oxide/Vycor Composite Membrane Structures by an Optimized LPCVD Process* , in publishing

4. Sherman, A., *Chemical Vapor Depositionfor Microelectronics,* Noyes Publications: New Jersey, 1987

5. Van den Brekel, C.H.J., *Chemical Vapor Deposition*, Blocher, J. M.; Vuilland, G.E.; Wahl, G. Eds., The Electrochemical Society: Pennington , New Jersey, 1981

6. O'Mara, W. C.; Herring, R. B.; Hunt, L. P., *Handbook of Semiconductor Silicon Technology ,* Noyes Publications: New Jersey, 1990

7. Kern, W., In *Microelectronic Material and Processes,* R. A. Levy Eds., Kluwer Academic: New Jersey, 1986

8. Kern, W.; Schnable, G. L., *IEEE Trans. Electron Devices*, **1979**, *ED-26,* 647

9. Brown, W. A.; Kamins, T. I., *Solid State Technol.,* **1979**, *22*(7), 51

10. Hersce, S. D.; Duchemin, J. P., *Annu. Rev. Mater. Sci.,* **1982**, *12*, 65

11. Singer, P. H., *Semicond.Int.*, **1984,** *7*(5), 72; *7*(13), 82

12. Learn, A. J., J. *Electrochem. Soc.,* **1985**, *132,* 390

13. Kern, W. ; Schnable, G. C., *RCA Review*, **1982**, *43*, 423

14. Middlemann, S.; Yeckel,A., *J. Electrochem. Soc.*,**1986**, *133,* 1951

15. Stein, H. J. ; Wells, V. A.; Hampy, R. E. , *J. Electrochem. Soc.* , **1979**, *126*, 1750

16. Mukai, K.; Hivaiwa, A.; Muramatsu, S.; Takahashi, S.; Harada, W., *Electrochem. Soc. Ext. Abstr.*, **1979**, *79* (1), 268

17. Watanabe, K.; Tanigaki, T.; Wakayama, S., *J. Electrochem. Soc.*, **1981**,*128*, 2630

18. Rosler, R. S., *Solid State Technol.*, **1977**,*20*(4), 63

19. Goldsmith, N.; Kern, W., *RCA Rev.* **1967**, *28*, 153

20. Cobianu, C.; Pavelescu, C., *J. Electreochem. Soc.*, **1983**, *130*, 1888

21. Cobianu, C, Pavelescu, C., *Thin Solid Films*, **1984**, *117*, 211

22. Becker, F. S.; Pawlick, D.; Schafer, H.; Standigl, G., *J. Vac. Sci. Technol.*, **1986**, ***B4***(3), 732

23. Huppertetz, H.; Engl, W. L., *IEEE Trans. Electron Devices*, **1979**, *ED-26*, 658

24. Hochberg, A. K.; Lagendijk, A.; O'Meara, D. L.; Klerer,J., *J. Electrochem. Soc.* , **1961**, *108*, 1070

25. Jordan , E. L., *ibid.*, **1961**, *108*, 478

26. Klereer, j., *ibid.*,**1965**, *112*(5), 503

27. Hochberg, A. K.; O'Meara, D. L., *ibid.*, **1989**, *136* (6), 1843

28. Orshonik, J.; Kraitchman, J., *ibid.*, **1968**, *115*, 649

29. Levy, R. A.; Gallagher, P. K.; Schrey, F., *ibid.*, **1987**, *134*, 430; 1744

30. Albella, J. M.; Criado, A.; Muroz Merino, E., *Thin Solid Films*, **1976**, *36*, 479

31. Levy , R. A.; Grow, J. M.; Chakravarthy, G. S., *Chem. Mater.*, **1993**, *5*, 1710

32. Huo, D. T. C.; Yan, M. F.; Foo, P. D.; *J. Vac. Sci. Technol.*, 1991, *A9*, (5), 2602

33. Patterson, J. D.; Ozturk, M. C., *ibid.*, **1992**, *B10*(2), 625

34. Gelerrt, B., *Semicond. Int.*, **1990**, *13*, 83

35. Hochberg, A. K.; Lagendijk, A.; O'Meara, D. L.; *J. Electrochem. Soc. Ext. Abstr.*, **1988**, *88-2*, 335

36. Adams , A. C.; Capio, C.D.; *J. Electrochem. Soc.*,**1979**,*126*, 1042

37. Adams, A. C.; Alexander, F. B.; Capio, C. D.; Smith, T. E., *ibid.*, **1981**, *128*, 1545

38. Emesh, T.; D'Asti, G.; Mercier, J. S.; Leung, P., *ibid.*, **1989**, *136*, 3404

39. Fracassi, F.; D'Agostino, R.; Favia, P., *ibid.*, **1992**, *139*, 2636

40. Evert, P. G. T. Van de ven, *Solid State Technol.*, **1981**, *24*(4), 167

41. Mackens, U.; Merkt, U., *Thin Solid Films*, **1982**, *97*, 53

42. Chin, B.L.; Evert, P. G. T. Van de ven, *Solid State Technol.*, **1988**, *31*(4), 119

43. Gorthy, C. S., *Low Temperature Synthesis and Characterization of LPCVD Silicon Dioxide Films Using Diethylsilane*, MS. Thesis, New Jersey Institute of Technology, Newark, New Jersey, 1992

44. Datta, A., *Synthesis of Silicon Oxide/Vycor Composite Membrane Structures by an Optimized LPCVD Process,* MS. Thesis, New Jersey Institute of Technology, Newark, New Jersey, 1995

45. Grow, J. M.; Levy, R. A.; Yu, Y.; Shih, K. T., *Mat. Res. Symp. Proc.*, **1994**, 344, 241

46. Wong, J., *J. Electron. Mater.*, **1976**, *5*(2), 113-160

47. Pliskin, W. A., *Semiconductor.Silicon*, Huff, H. R.; Burgess, R. R.*Eds.,* Electrochem. Soc., Princeton, New Jersey, 1973, p506

48. Kobeda, E.; Kellom,M.; Psburn, C.M; *J.Electrochem.Soc.*,**1991,***138*(6), 1846

49. Taylor, S.; Zhang, J.F.; Eccleston, W., *Semicond. Sci. and Technol.*, **1993**, *8* (7), 1426

50. Chapple-Sokol, J.D.; Pliskin, W.A.; Conti, R.A, *J.Electrochem.Soc*, 1991, *138*(12), 3723

51. Ceiler, M.F. Jr.; Kohl, P.A.; Bidstrup, S.A., *ibid.*, **1995**, *142*(6), 2067

52. Fracassi, F., d'Agostino, R.; Favia, P., *ibid.*, **1992**,*139*(9), 2636

53. Pai, C S.; Chang, C.P.; *J.Appl. Phys.*, **1990**,*68*, 793

54. Chang, C.P.; Pai, C.S.; Hiseh, J.J., *ibid.*, **1990**,*67*, 2119

55. Veprek-Heijman, M. G. J.; Bontand, D., *J. Electrochem. Soc.* **1991**, *138*, 2042

56. Smith, D. L.; Alimonda, A. S., *ibid.*, **1993**, *140*, 1496